

Disentangling Uncertainty for Safe Social Navigation using Deep Reinforcement Learning

Daniel Flögel^{*1}, Marcos Gómez Villafañe^{*1,2}, Joshua Ransiek¹, and Sören Hohmann³

Abstract—Autonomous mobile robots are increasingly used in pedestrian-rich environments where safe navigation and appropriate human interaction are crucial. While Deep Reinforcement Learning (DRL) enables socially integrated robot behavior, challenges persist in novel or perturbed scenarios to indicate *when and why* the policy is uncertain. Unknown uncertainty in decision-making can lead to collisions or human discomfort and is one reason why safe and risk-aware navigation is still an open problem. This work introduces a novel approach that integrates *aleatoric*, *epistemic*, and *predictive* uncertainty estimation into a DRL navigation framework for policy distribution uncertainty estimates. We, therefore, incorporate Observation-Dependent Variance (ODV) and dropout into the Proximal Policy Optimization (PPO) algorithm. For different types of perturbations, we compare the ability of deep ensembles and Monte-Carlo dropout (MC-dropout) to estimate the uncertainties of the policy. In uncertain decision-making situations, we propose to change the robot’s social behavior to conservative collision avoidance. The results show improved training performance with ODV and dropout in PPO and reveal that the training scenario has an impact on the generalization. In addition, MC-dropout is more sensitive to perturbations and correlates the uncertainty type to the perturbation better. With the safe action selection, the robot can navigate in perturbed environments with fewer collisions.

I. INTRODUCTION

Autonomous mobile robots are increasingly being deployed in a variety of public pedestrian-rich environments, e.g. pedestrian zones for transport or cleaning [1]–[3], while DRL-based approaches are increasingly used [3, 4]. These robots not only have socially aware behavior but also become socially integrated to reduce the negative impact on humans [5]. However, there are two fundamental challenges. The first arises through the variety and a priori unknown scenarios caused by the stochastic behavior of humans [6, 7]. The second through the general problem of machine learning-based systems to predict correct actions in unseen scenarios [8, 9]. Since the robot has to choose an action in each step, one risk is a high level of uncertainty in the decision-making process at action selection [10]. As a consequence, safe and risk-aware social navigation to avoid collisions and human discomfort is still an open problem [3, 11].

The uncertainty in the robot’s decision-making is affected by scenarios the robot has never experienced in training,

^{*} Authors contributed equally: Daniel Flögel, Marcos Gómez Villafañe
¹ are with FZI Research Center for Information Technology, Karlsruhe, Germany floegel@fzi.de

² is with Facultad de Ingeniería, Universidad de Buenos Aires, Buenos Aires, Argentina

³ is with the Institute of Control Systems at Karlsruhe Institute of Technology, Karlsruhe, Germany soeren.hohmann@kit.edu

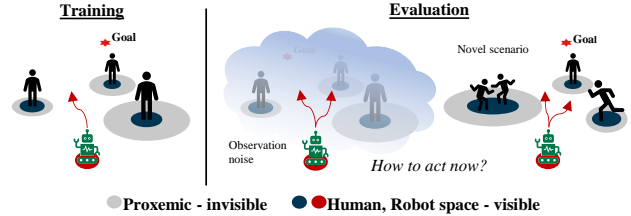


Fig. 1: We propose to integrate aleatoric and epistemic uncertainty estimation of action selection into DRL-based navigation policies to detect scenarios where the robot is uncertain, e.g. due to observation noise or novel scenarios. Depending on the confidence about action selection, the robot either interacts with humans or focuses on safe collision avoidance.

Out-Of-Distribution (OOD) scenarios, and due to the inherent uncertainty of the environment like sensor noise or occlusion [12]. Thus, the DRL policy will face *epistemic uncertainty* (model uncertainty), which correlates with OOD, and *aleatoric uncertainty*, which stems from stochastic environments, e.g. sensor noise or perturbations on selected actions [13]. For a DRL policy, it is essential to estimate both types as it is expected that the robot identifies anomalous environmental states if it does not know which action to take to account for potential risks [13, 14]. Thus, disentangling aleatoric and epistemic uncertainty is crucial for a DRL policy towards safe and risk-aware behavior [14]. However, there is less literature on uncertainty aware DRL, compared to supervised learning [15], and only a few works address the resulting risks in social navigation [16].

Most DRL-based navigation approaches, e.g. [5, 17]–[21], do not consider OOD scenarios or noise, which is a significant risk since the OOD performance of recent approaches is poor as evaluated in [3]. For known input perturbations, a certified adversarial robustness analysis framework for DRL is proposed in [10]. However, the perturbation must be known a priori, and it only applies to DRL approaches with discrete actions. Other recent works make use of the uncertainty in the human trajectory prediction [1, 4] or propose to detect novel scenarios [9]. However, these approaches neglect the uncertainty in decision-making, which is the crucial part [10]. In addition, [9] intentionally replaced PPO [22] with Soft Actor-Critic (SAC) [23] because standard implementations, e.g. *Stables Baselines3* [24], of PPO do not have state dependant variance of policy distribution and it is additionally challenging for PPO to train uncertainty-aware behavior while having good exploration-exploitation trade-off. However, many social navigation approaches rely on the PPO algorithm due to the stable training and good performance, e.g. [2, 4, 5, 12, 25]–[30].

We see the clear limitation that the uncertainty in the

policy distribution is neither considered nor is the source of the uncertainty determined. Thus, we propose to disentangle the policy’s uncertainty measures and to adapt the robot’s interaction behavior according to the confidence in decision-making, as it is essential for successful deployment in real-world environments [13, 15].

As the main contributions of this work, (i) we extend the PPO algorithm with Observation-Dependent Variance (ODV) and ensure stable training with an additional loss function and variance clamping. (ii) On top of that, we compare the capability of MC-dropout and deep ensembles to disentangle the uncertainty estimates of the policy distribution and incorporate predictive uncertainty estimation into the feature extractor. (iii) Based on the uncertainty estimates, we use a parametrized function to detect high-risk scenarios and change the robot’s social interaction behavior to reduce collisions. We conduct the experiments in simulation to evaluate the algorithms’ response to dynamic obstacles in a reproducible environment and investigate the impact of training scenarios on generalization, as we consider this as an essential prior step for real-world experiments.

II. BACKGROUND

A. Uncertainty Estimation in Machine Learning

Estimating the uncertainty can be distinguished into sample-free and sample-based methods, e.g., MC-dropout or ensembles, which require multiple forward passes [31]. Ensemble methods consist of multiple models trained with different weight initializations. The variance of the different model predictions can be considered as Bayesian uncertainty estimates [31]. MC-dropout, which uses dropout during testing as regularization, randomly drops neurons in testing to form different models and combine their predictions as Bayesian uncertainty estimation [32]. The uncertainty estimates can be further distinguished into aleatoric, epistemic, and predictive uncertainty [15, 33]. Aleatoric uncertainty arises from the stochastic nature of the environment and can not be reduced. The three main sources in DRL are stochasticity in observation, actions, and rewards [15]. Epistemic uncertainty arises from limited knowledge gathered in training and accounts for the lack of knowledge of a policy but can be reduced with more training samples [15, 31]. Predictive uncertainty summarizes the effects of aleatoric and epistemic uncertainty [33, 34]. The literature for uncertainty-aware DRL includes Bayesian DRL [35] such as an ensemble [36] or dropout [37] approaches. However, only a few methods aim to disentangle the uncertainty estimation in action selection [15]. For the Double Q-Network (DQN) algorithm, aleatoric and epistemic uncertainty are disentangled in [13, 14] but not adapted for actor-critic algorithms with continuous action space such as PPO which is challenging [9]. The sample-based approximations, MC-dropout and ensembles, require the least changes to the PPO algorithm, but challenges arise for aleatoric estimates as it requires an observation-dependent variance in policy distribution, which is not the case for the PPO algorithm and not necessarily boosts training performance. In DRL, dropout is also not

a common choice due to the non-stationary targets [15], and naive application can be challenging for PPO [38]. In addition, a benchmark of different uncertainty estimation methods for a classification task shows that disentangling the uncertainties remains an unsolved problem and concludes that tailored methods for specific tasks are needed [34]. Thus, disentangling uncertainty estimates and incorporating them into DRL is an ongoing field of research.

B. Safety in Social Navigation

DRL-based social navigation approaches can be categorized based on the robot’s exhibited social behavior in human-machine interaction into Social Collision Avoidance (SCA) with a lack of social aspects, Socially Aware (SA) approaches with a predefined social behavior, and Socially Integrated (SI) where the robot’s behavior is adaptive to human behavior and emerges through interaction [5]. For a more detailed description of core challenges in social navigation is referred to [3], for the proxemics in social navigation to [39], and how social behavior emerges to [5].

For safety in social navigation, early works proposed a Probability of Collision (POC) distribution in combination with a model-predictive controller (MPC) for safe and uncertainty-aware action selection [36, 37]. [37] uses MC-dropout and bootstrapping to estimate the POC distribution for a risk-aware exploration in model-based DRL. An ensemble of LSTMs is used in [36] in combination with MC-dropout and bootstrapping to estimate the distribution. A risk function is proposed in [2] to capture the POC to prioritize humans with a higher risk of collision. However, a learned POC can be uncertain and does not reflect the policy uncertainty in the action selection. Other approaches use the uncertainty in human trajectory prediction for risk-aware planning [1, 4]. Such approaches are highly susceptible to the stochasticity of noise, and the unobserved intentions of the external agents, which is addressed in [40] with a model-based DRL approach by estimating the aleatoric uncertainty of the trajectory prediction. A risk-map-based approach with human position prediction and probabilistic risk areas instead of hard collision avoidance is proposed in [11] to address dynamic human behavior and static clutter. Other works propose safety zones around humans, e.g. [20, 41], to increase the minimum distance between the robot and humans. To overcome the problem of occluded humans, the social inference mechanism with a variational autoencoder to encode human interactions is incorporated in [12]. A risk-conditioned distributional SAC algorithm that learns multiple policies concurrently is proposed in [16]. The distributional DRL learns the distribution over the return and not only the expected mean, and the risk measure is a mapping from return distribution to a scalar value. Other work estimate uncertainty from environmental novelty [42], which does not translate to policy uncertainty. A resilient robot behavior for navigation in unseen uncertain environments with collision avoidance is addressed in [9]. An uncertainty-aware predictor for environmental uncertainty is proposed to learn an uncertainty-aware navigation network

in prior unknown environments.

In summary, there are no existing model-free DRL approaches disentangle and consider the policy distribution uncertainty in action selection, which is crucial for safe and risk-aware decision-making.

III. PRELIMINARIES

A dynamic object in the environment is generally referred to as an agent, either a robot or a human, and a policy determines its behavior. Variables referred to the robot are indexed with x^0 , and humans with x^i with $i \in 1, \dots, N - 1$. A scalar value is denoted by x and a vector by \mathbf{x} .

A. Problem Formulation

The navigation task of one robot toward a goal in an environment of $N - 1$ humans is a sequential decision-making problem and can be modeled as Partially Observable Markov Decision Process (POMDP) and solved with a DRL framework [43]. The POMDP is described with a 8-tuple $(\mathcal{S}, \mathcal{A}, \mathcal{T}, \mathcal{O}, \Omega, \mathcal{T}_0, R, \gamma)$. We assume the state space \mathcal{S} and action space \mathcal{A} as continuous. The transition function $\mathcal{T} : \mathcal{S} \times \mathcal{A} \times \mathcal{S} \rightarrow [0, 1]$ describes the probability transitioning from state $\mathbf{s}_t \in \mathcal{S}$ to state $\mathbf{s}_{t+1} \in \mathcal{S}$ for the given action $\mathbf{a}_t \in \mathcal{A}$. With each transition, an observation $\mathbf{o}_t \in \mathcal{O}$ and a reward $R : \mathcal{S} \times \mathcal{A} \rightarrow \mathbb{R}$ is returned by the environment. The observation \mathbf{o}_t is returned with probability $\Omega(\mathbf{o}_t | \mathbf{s}_{t+1}, \mathbf{a}_t, \mathbf{s}_t)$ depending on the sensors. The initial state distribution is denoted by \mathcal{T}_0 while $\gamma \in [0, 1)$ describes the discount factor. Every agent is completely described with a state $\mathbf{s}_t^i = [\mathbf{s}_t^{i,o}, \mathbf{s}_t^{i,h}]$ at any given time t . The state is separated into two parts. The observable part $\mathbf{s}_t^{i,o} = [\mathbf{p}, \mathbf{v}, r]$ is composed of position \mathbf{p} , velocity \mathbf{v} , and radius r . The unobservable, hidden part, $\mathbf{s}_t^{i,h} = [\mathbf{p}_g, v_{\text{pref}}, \psi_{\text{pref}}, r_{\text{prox}}]$ is composed of goal position \mathbf{p}_g , preferred velocity v_{pref} , preferred orientation ψ_{pref} , and a proxemic radius r_{prox} according to Hall’s proxemic theory [44]. The world state $\mathbf{s}_t = [\mathbf{s}_t^0, \dots, \mathbf{s}_t^{N-1}]$ represents the environment at time t . One episode’s trajectory τ is the sequence of states, observations, actions, and rewards within the terminal time T . The return of one episode $\mathcal{R}(\tau) = \sum_{t=0}^T \gamma^t R_t$ is the accumulated and discounted reward R_t . The central objective is to learn the optimal robot policy π^* which maximizes the expected return:

$$\mathcal{T}(\tau | \pi) = \mathcal{T}_0 \prod_{t=0}^T \mathcal{T}(\mathbf{s}_{t+1} | \mathbf{s}_t, \mathbf{a}_t) \pi(\mathbf{a}_t | \mathbf{o}_t), \quad (1)$$

$$\mathbb{E}_{\tau \sim \pi} [\mathcal{R}(\tau)] = \int_{\tau} \mathcal{T}(\tau | \pi) R(\tau), \quad (2)$$

$$\pi^*(\mathbf{a} | \mathbf{o}) = \arg \max_{\pi} \mathbb{E}_{\tau \sim \pi} [\mathcal{R}(\tau)]. \quad (3)$$

Considering a stochastic environment, $\mathcal{T}(\tau | \pi)$ is the probability of a trajectory starting in \mathbf{s}_0 with \mathcal{T}_0 .

We follow our previous framework in [5] to train a SI navigation policy and use the same reward and observation system. The policy is trained from scratch, respects proxemic and velocity social norms, and exhibits social behavior that is adaptive to individual human preferences. The action of the policy is a velocity v_t and delta heading $\Delta \theta_t$ command.

IV. APPROACH

This section describes our framework for safe action selection using disentangled uncertainty estimates of a DRL navigation policy. The framework is composed of three main components. A navigation policy that predicts uncertainties along the actions, a time step-based risk assessment, and a safe action selection. First, we introduce Observation-Dependent Variance (ODV) into the PPO algorithm to enable aleatoric uncertainty estimates. Subsequently, we describe aleatoric, epistemic, and predictive uncertainty estimation in the DRL policy using MC-dropout and deep ensembles. Finally, we provide a Probability of Collision (POC) estimation based on the uncertainty estimates and change the robot’s navigation strategy into cautious SCA for risk-aware action selection in novel and perturbed environments.

A. Observation-Dependent Variance

In standard implementations of PPO, e.g. *Stables Baselines3* [24], the actor outputs multivariate Gaussian distributed actions $\mathcal{N}(\boldsymbol{\mu}_a(\mathbf{o}_t), \boldsymbol{\sigma}_a^2)$ with an observation dependent mean but a parameterized variance, independent from observation. An observation-independent variance does not allow for aleatoric uncertainty estimation of the action selection process [9]. Therefore, the actor network is adapted, and a linear layer is incorporated to output the observation-dependent variances for the actions as $\log(\boldsymbol{\sigma}_a)$. This leads to a multivariate Gaussian distributed policy $\mathcal{N}(\boldsymbol{\mu}_a(\mathbf{o}_t), \boldsymbol{\sigma}_a^2(\mathbf{o}_t))$ where both the mean and variance of the policy depend on the observation. However, using ODV leads to stability problems during training. First, the variance can be arbitrarily large, which can cause the normal distribution to lose its shape, become a uniform distribution, and disrupt learning because actions are sampled randomly. Second, policy updates can lead to high variances at the late stages of training, which, by sampling, may lead to a sequence of poor actions, a series of bad updates, and, finally, performance collapse. We propose to use variance clamping for the first problem to prevent the deformation of the normal distribution by limiting the maximum variance. A grid search for the clamping values was done, and the highest maximum clamping value that did not cause collapse and still resembled a normal distribution is used. The second problem is addressed by modifying the PPO loss by adding a Mean Squared Error (MSE) loss for the action variance

$$\mathcal{L}_{\theta}^{\sigma}(\pi) = \frac{t}{T} \cdot \lambda_{\sigma} \cdot \frac{1}{B} \sum_{i=1}^B \frac{1}{2} \cdot \|\boldsymbol{\sigma}_a^2 - \boldsymbol{\sigma}_{\text{tgt}}^2\|^2, \quad (4)$$

where $\frac{t}{T}$ accounts for exploration-exploitation trade-off with the current timestep t and the total training timesteps T and batch size of B . The constant λ_{σ} scales and weights the variance loss, and $\boldsymbol{\sigma}_{\text{tgt}}^2$ is a desired target variance for each action. This leads to total policy loss $\mathcal{L}_{\theta}(\pi) = \mathcal{L}_{\theta}^{\text{CLIP}}(\pi) + \mathcal{L}_{\theta}^{\sigma}(\pi)$ where $\mathcal{L}_{\theta}^{\text{CLIP}}(\pi)$ is the PPO clipping loss. We refer to the full model as Observation-Dependent Variance PPO (ODV-PPO).

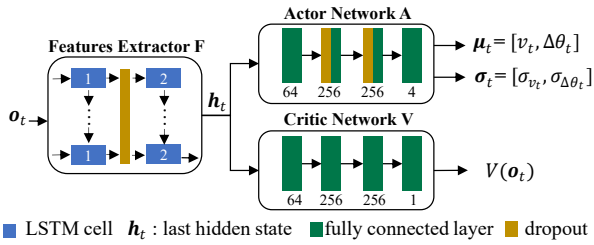


Fig. 2: Our ODV-PPO network, a common actor-critic architecture, with a shared features extractor and separated actor and value networks. The actor and the features extractor contain dropout layers. The actor outputs an observation-dependent mean and variance.

B. Uncertainty Estimation

1) *MC-Dropout*: We incorporate dropout to approximate Bayesian inference in deep Gaussian processes, referred to as MC-dropout [32]. Implemented in two parts of the ODV-PPO network, in the 2-layer LSTM features extractor and in the hidden layers of the actor-network, as depicted in Fig. 2. The critic network does not contain a dropout to avoid instabilities in the target value [15]. The policy is first trained with dropout probability p_{train} . In the testing phase, the samples are drawn with a higher dropout p_{test} to estimate the uncertainty. We sample K independent policy predictions with dropout of the action distribution $\mu_k, \sigma_k = \pi(\cdot | o_t)$ for an observation at time step t . Subsequently, we calculate the uncertainties as proposed in [14] from the individual samples. The epistemic uncertainty is estimated with the variance of the means with

$$\mathbf{u}^{\text{ep}} = \mathbb{V}[\boldsymbol{\mu}] \approx \frac{1}{K} \sum_{k=1}^K (\boldsymbol{\mu}_k - \bar{\boldsymbol{\mu}}_k)^2, \quad (5)$$

where $\bar{\boldsymbol{\mu}}_k$ is the average of the mean predictions obtained with dropout at time t . Additionally, we calculate the mean over the variances, which represents the aleatoric uncertainty

$$\mathbf{u}^{\text{al}} = \mathbb{E}[\boldsymbol{\sigma}^2] \approx \frac{1}{K} \sum_{k=1}^K \boldsymbol{\sigma}_k^2. \quad (6)$$

Both uncertainty estimates are vectors with the dimension of the action space.

2) *Deep Ensembles*: For deep ensembles, K networks are trained separately with different weight initialization and in environments with different seeds. A single network in the ensemble has the same architecture as in Fig. 2 and is trained in the same way as for MC-dropout. The dropout is used in the training for regularization but not used to calculate uncertainty estimates. In testing, each model of the ensemble gets the same observation. Thus, we generate K independent samples of the mean and variance of the actions. The epistemic uncertainty is then calculated with (5) and the aleatoric with (6).

3) *Features Extractor Uncertainty*: In addition to the epistemic and aleatoric uncertainty in the actor network, we estimate the predictive uncertainty of the features extractor, which does not distinguish between aleatoric and epistemic uncertainty. We distinguish between the predictive features

uncertainty estimation with MC-dropout and with the deep ensembles method.

For MC-dropout, we get K samples of the hidden state \mathbf{h}_t at each time step t to estimate the uncertainty. Based on the K features vectors, we estimate a degree of uncertainty based on the method proposed in [45] and based on the element-wise variance in the features vector \mathbf{h}_t at each time step. This features variance vector is

$$\mathbb{V}(\mathbf{h}) = \begin{bmatrix} \mathbb{V}[h_1] \\ \vdots \\ \mathbb{V}[h_D] \end{bmatrix} = \begin{bmatrix} \frac{1}{K} \sum_{i=1}^K (h_{1,i} - \bar{h}_1)^2 \\ \vdots \\ \frac{1}{K} \sum_{i=1}^K (h_{D,i} - \bar{h}_D)^2 \end{bmatrix}, \quad (7)$$

where D is the dimension of \mathbf{h} and $h_{d,i}$ is the d -th features vector element of the i -th sample from the K forward passes, and $\bar{h}_d = \frac{1}{K} \sum_{i=1}^K h_{d,i}$ is the mean for each element over the samples. During training, the minimum and maximum of each element in the features vector are tracked as h_d^{min} and h_d^{max} . Based on these values, an upper bound of the variance $\mathbb{V}[h_d]^{\text{max}} = \frac{(h_d^{\text{max}} - h_d^{\text{min}})^2}{12}$ is calculated for each element, which occurs when the distribution follows a uniform distribution. Since the dimension of the features vector is commonly very high, a mapping function $g(\cdot) : \mathbb{R}^d \rightarrow \mathbb{R}$ is used to map the variance to a degree of uncertainty u^{feat} as proposed in [45]:

$$u^{\text{feat}} = g(\mathbb{V}(\mathbf{h})) = \sum_{d=1}^D \frac{\mathbb{V}(h_d)}{\sum_{d=1}^D \mathbb{V}(h_d)} \frac{\mathbb{V}(h_d)}{\mathbb{V}[h_d]^{\text{max}}}, \quad (8)$$

where $\mathbb{V}(h_d)$ is the d -th element of the features variance vector and $\mathbb{V}[h_d]^{\text{max}}$ is used to normalize the uncertainty.

For deep ensembles, the uncertainty mapping is performed with the average of the features uncertainty

$$u^{\text{feat}} = g(\mathbb{V}(\mathbf{h})) = \frac{1}{D} \sum_{d=1}^D \mathbb{V}(h_d). \quad (9)$$

Using (8) would require training the ensemble models in parallel in the same environment, which is computationally heavy for a large K .

C. Uncertainty-Aware Action Selection

To avoid collision in scenarios where the robot is uncertain in action selection, we use the uncertainty estimates for a POC estimation. For POC estimation, we investigated the usability of a sigmoid function, a Probability of Collision Network (PCN), and a threshold function, all with uncertainties as input. The sigmoid function could not be parameterized manually. The PCN, inspired by [36] additionally considers the temporal evolution and is trained in a supervised manner based on gathered DRL rollouts. However, the PCN only

TABLE I: ODV-PPO Hyperparameters

Parameter	Value	Parameter	Value
variance factor λ_σ	0.3	dropout rate p_{train}	0.1
target variance σ_{tgt}^2	0	dropout rate p_{test}	0.5
variance clamping min	-20	samples/models K	20
variance clamping max	0.25	learning rate	0.000 25
batch size	128	num steps	128

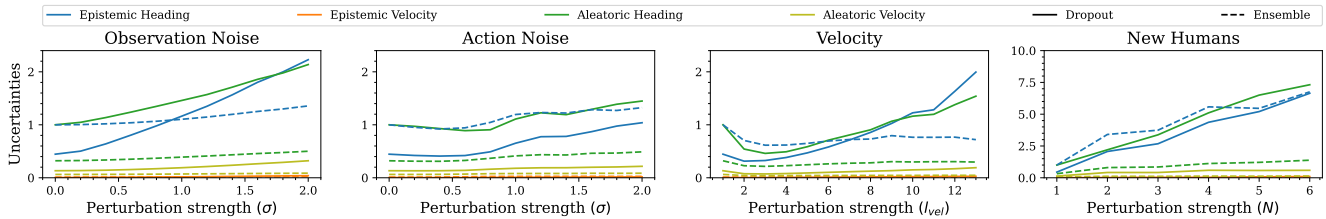


Fig. 3: Normalized and episodic mean values of epistemic and aleatoric uncertainty estimation using the MC-dropout and deep ensemble approach.

performed well for action noise in our experiments, and we could not claim the generalization of the PCN itself therefore, we decided on a white box approach for the POC since the risk assessment is an essential part for safe action selection. Thus, we use the threshold function

$$\mathbb{P}(\text{col}) = \begin{cases} 1, & \text{if } (c_{\text{ep}} \vee c_{\text{feat}}) \wedge c_{\text{prox}} \wedge c_{\text{ap}}, \\ 0, & \text{otherwise} \end{cases}, \quad (10)$$

which indicates if the uncertainty condition, distance analysis, and scenario measure turn true. The uncertainty conditions indicate if the heading epistemic $c_{\text{ep}} = \mathbb{1}[u_{\text{head}}^{\text{ep}} > \lambda_{\text{ep}}]$ or the predictive feature uncertainty $c_{\text{feat}} = \mathbb{1}[u_{\text{feat}}^{\text{ep}} > \lambda_{\text{f}}]$ are beyond a threshold. To analyze the trend of uncertainty in the trajectory, we smooth the noisy step-wise uncertainty estimates by windowing them over w previous steps. The proximity condition flags $c_{\text{prox}} = \mathbb{1}[(d_t^{0,j} + \beta_1 \cdot |\Delta v_t^{0,j}|) < \lambda_{\text{prox}}]$ scenarios with the close distance $d_t^{0,j}$ to another human and takes into account the relative velocity $\Delta v_t^{0,j}$ to the nearest human. The approach condition $c_{\text{ap}} = \mathbb{1}[d_{t-1}^{0,j} \leq d_t^{0,j}]$ considers that once the robot is moving away from the human, the risky scenario was averted.

With the POC, a risk-aware action selection can be proposed by either reducing the velocity or using a cautious policy when the POC is high. Since reducing the velocity is not always safe when humans move fast [36], we use a cautious policy. According to the social navigation taxonomy in [5], we propose to change the robot’s interaction behavior to a SCA strategy in high-risk scenarios instead of a SA or SI strategy and focus on physical collision avoidance in the first regard. As a collision avoidance strategy, we use the Optimal Reciprocal Collision Avoidance (ORCA) [46] model. To increase the caution, the radius of the surrounding humans is assumed to be 1.5 times bigger as observed, promoting trajectories away from humans and considering a safety zone.

V. EVALUATION

We follow the principles and guidelines of evaluating social navigation [47] and evaluate the algorithm’s response to dynamic obstacles in a reproducible simulation environment as a prior step of real-world experiments. First, we compare the training and generalization performance of the proposed ODV-PPO algorithm in different scenarios. Subsequently, we compare the capability of MC-dropout and deep ensembles to disentangle different types of perturbations. Finally, we investigate the suitability of the uncertainty estimates to detect risky scenarios and avoid collisions.

A. Experimental Setup

We use the simulation environment from our previous work in [5] with microscopic and social-psychological interaction behavior and *Stables Baselines3* [24] to train and evaluate all policies. For PPO with and without dropout, we use the optimized hyperparameters from [5]. For all ODV-PPO variants, we adapted the hyperparameters based on Optuna [48] hyperparameter search, as stated in Table I.

To evaluate the design choices of the ODV-PPO and the impact of dropout, we consider three different scenarios: a circle-interaction [5], a circle crossing, and a random scenario. In all scenarios, the agents’ preferred speed and human’s proxemic radius are sampled from $\mathcal{U}[0.5, 1.0]$ and $\mathcal{U}[0.3, 0.7]$, respectively. The start and goal positions are randomly sampled within the red areas, as depicted in Fig. 5 and the robot is randomly assigned to one of the blue start-goal pairs. In each scenario, we train 15 policies per algorithm across different seeds and evaluate each policy for 200 episodes in all scenarios to investigate the generalization.

We train new policies for uncertainty estimation and consider a position swap scenario where the human position is randomly sampled on a circle with 7 m radius. All policies are trained in this simple position swap scenario with one human, and the human proxemic radius is sampled with $r_{\text{prox}} = \mathcal{U}(0.3, 0.4)$. To analyze the uncertainty estimates, the position swap scenario is systematically expanded with perturbations, noise, and more humans. We stimulate aleatoric uncertainty with observation and action noise and epistemic uncertainty with an increased velocity of humans and an increased number of humans. Observation noise is modeled with additive Gaussian noise $\mathcal{N}(0, I \cdot \sigma_{\text{obs}}^2)$. Action noise for the heading is modeled with additive Gaussian noise $\mathcal{N}(0, \sigma_{\text{head}}^2)$ and the velocity is scaled with a uniformly sampled factor $\mathcal{U}(1 - \sigma_{\text{vel}}, 1)$ with $\sigma_{\text{vel}} \leq 1$ to simulate terrain grip and avoid actions with negative velocity. The epistemic uncertainty is introduced through scaling the preferred velocity $l_{\text{vel}} \cdot v_{\text{pref}}^i$ of humans and adding multiple humans into the environment to extend the position swap scenario into a circle-crossing scenario.

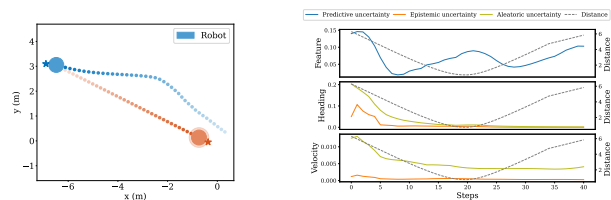


Fig. 4: Windowed uncertainty estimates ($w = 4$) using MC-dropout approach. Position swap scenario with start and goal position perturbation.

TABLE II: Aggregated evaluation results across 15 seeds with 200 evaluation episodes per scenario and seed. Goal, Return: \uparrow ; Coll., Time out \downarrow

Training Scenario	Algorithm	Eval. Scenario: Circle Interaction				Eval. Scenario: Circle Crossing				Eval. Scenario: Random			
		Goal (%)	Col. (%)	Time out (%)	Return ($\mu \pm \sigma$)	Goal (%)	Col. (%)	Time out (%)	Return ($\mu \pm \sigma$)	Goal (%)	Col. (%)	Time out (%)	Return ($\mu \pm \sigma$)
Circle Interaction	PPO	99.80	0.20	0.00	4.5 \pm 0.46	93.30	4.37	2.33	3.66 \pm 2.09	76.80	4.70	18.50	2.63 \pm 3.63
	PPO-Drop	99.90	0.10	0.00	4.66 \pm 0.42	94.40	3.83	1.77	3.92 \pm 2.01	78.70	5.40	15.90	2.93 \pm 3.65
	ODV-PPO no Loss	99.47	0.53	0.00	4.25 \pm 0.65	88.57	8.73	2.70	2.94 \pm 2.64	79.27	7.37	13.37	2.22 \pm 3.59
	ODV-PPO	99.23	0.77	0.00	4.29 \pm 0.78	89.93	7.80	2.57	3.12 \pm 2.55	77.77	7.50	14.73	2.15 \pm 3.79
	ODV-PPO-Drop	99.90	0.10	0.00	4.52 \pm 0.36	96.87	2.47	0.67	4.04 \pm 1.45	82.00	4.50	13.50	3.02 \pm 3.39
Circle Crossing	PPO	49.57	12.20	38.23	-1.25 \pm 5.16	86.10	7.07	6.83	2.17 \pm 3.49	58.90	7.83	33.27	-0.57 \pm 5.39
	PPO-Drop	87.80	1.13	11.07	3.15 \pm 2.78	98.13	1.57	0.30	3.91 \pm 1.24	82.33	4.07	13.60	2.71 \pm 3.61
	ODV-PPO no Loss	41.57	9.43	49.00	-2.28 \pm 4.98	71.47	2.03	26.50	0.83 \pm 4.45	40.80	8.63	50.57	-2.74 \pm 5.3
	ODV-PPO	38.37	6.67	54.97	-2.24 \pm 5.42	58.90	8.70	32.40	0.18 \pm 4.84	39.60	7.17	53.23	-2.51 \pm 5.87
	ODV-PPO-Drop	92.90	0.67	6.43	3.78 \pm 2.35	99.10	0.83	0.07	4.22 \pm 0.88	88.07	2.10	9.83	3.46 \pm 3.14
Random	PPO	68.03	5.60	26.37	1.36 \pm 4.39	68.40	8.60	23.00	1.15 \pm 4.12	80.40	2.37	17.23	2.44 \pm 3.80
	PPO-Drop	91.67	2.43	5.90	3.4 \pm 2.59	86.70	8.13	5.17	2.76 \pm 3.12	90.20	3.30	6.50	3.28 \pm 2.86
	ODV-PPO no Loss	0.00	0.37	99.63	-6.53 \pm 0.37	0.00	0.10	99.90	-6.54 \pm 0.71	0.00	0.10	99.90	-6.39 \pm 0.80
	ODV-PPO	58.50	2.20	39.30	0.19 \pm 4.81	53.53	3.30	43.17	-0.26 \pm 4.62	59.53	1.17	39.30	0.36 \pm 4.80
	ODV-PPO-Drop	99.53	0.30	0.17	4.33 \pm 0.74	97.53	2.43	0.03	4.04 \pm 1.33	99.43	0.47	0.10	4.39 \pm 0.83

B. Results

1) *Training and Generalization:* The training rewards in Fig. 5 and aggregated evaluation results in Table II show that naively adding ODV into PPO does not lead to good training and evaluation results or even to non-convergence. The newly introduced loss function in (4) stabilizes the training convergence behavior, but the evaluation results are worse than for PPO. In all scenarios, PPO with dropout improved training rewards and the generalization performance to out-of-distribution scenarios (scenarios the policy is not trained on). However, the combination of dropout and ODV-PPO leads to the best training rewards and evaluation results except for the circle interaction in-distribution scenario evaluation (same training and evaluation scenario) for the circle-interaction scenario. In all scenarios, ODV-PPO with dropout shows the best generalization performance to out-of-distribution scenarios, has the highest success rate (reached goal), and has the least collisions. All policies trained in the circle-interaction scenario converge very fast, have low variance throughout the seeds, and have good generalization results compared to those trained on circle crossing or random scenarios. Except for ODV-PPO with dropout, the evaluation results for these policies show even higher evaluation reward in the out-of-distribution scenarios, circle crossing and random, compared to the policies trained in these scenarios. Only PPO with dropout trained in the random scenario has a slightly higher in-distribution evaluation reward.

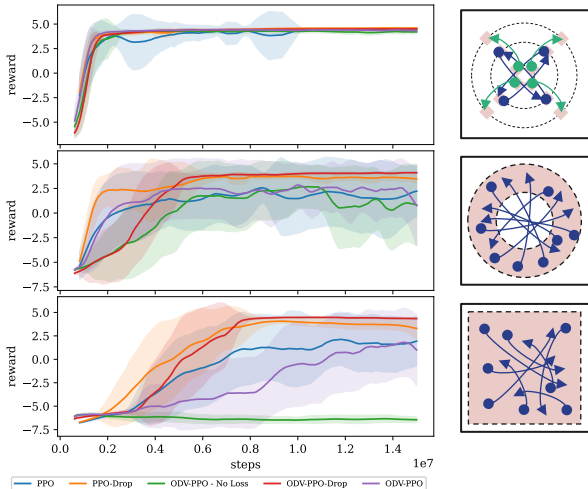


Fig. 5: Training reward across 15 seeds for different algorithms and scenarios. The agents goal and start positions are sampled in red areas.

2) *Disentangling Uncertainty Estimation:* We evaluate the MC-dropout and Deep Ensemble approach with different perturbation sources and strengths and estimate the uncertainties in each step. Observation and action noise is $\sigma_{\text{head}}, \sigma_{\text{vel}}, \sigma_{\text{obs}} \in [0, 0.2, \dots, 2]$, velocity scaling factor is $l_{\text{vel}} \in [1, \dots, 8]$, and new humans are $N \in [2, \dots, 7]$. The estimated aleatoric and epistemic uncertainties are depicted in Fig. 3. For both approaches, the results show that the velocity uncertainty is low and flat compared to the heading uncertainty, which increases approximately linearly, and new humans cause the highest uncertainty. In addition, the MC-dropout approach is capable of disentangling the source of the uncertainty, but we also observed that a proper dropout rate p_{test} is crucial for this capability. In contrast, the deep ensemble approach always has high epistemic uncertainty and cannot distinguish between aleatoric and epistemic uncertainty. The results are also aggregated in Table III for the normalized rate of change of the uncertainties for the perturbation. The normalized value is $\frac{\Delta U}{\Delta \sigma} = \frac{1}{u_{\sigma(0)}} \frac{u_{\sigma(\text{max})} - u_{\sigma(0)}}{\sigma(\text{max}) - \sigma(0)}$ with the maximum perturbation strength $\sigma(\text{max})$, the mean uncertainty $u_{\sigma(\text{max})}$ per strength, and the mean uncertainty $u_{\sigma(0)}$ in the unperturbed environment of the episodes.

To analyze the trend of uncertainty as the robot approaches and interacts with the human, the mean uncertainty \bar{u}_w over a window of the last $w = 4$ steps is evaluated. The experiments show that the predictive uncertainty increases for both approaches in close situations, as exemplified in Fig. 4, but the action uncertainty is low. For MC-dropout approach, the windowed predictive feature uncertainty is one step before collision (if occurred) higher for action and velocity noise compared to the step of minimum distance (if no collision occurred), as depicted in Fig. 6. However, there is no distinction for the deep ensemble approach, which is additionally less sensitive. In addition, the results show that the number of collisions increases with the perturbation strength, as depicted with grey dots in Fig. 6.

TABLE III: Normalized aggregated uncertainty estimates.

Uncertainties	Observation Noise		Action Noise		Velocity		New Humans	
	Dropout	Ensemble	Dropout	Ensemble	Dropout	Ensemble	Dropout	Ensemble
Predictive Feature	1.84	0.11	0.87	0.03	0.20	0	0.65	0.38
Aleatoric Heading	0.57	0.28	0.22	0.26	0.04	0	0.90	0.47
Epistemic Heading	2.00	0.18	0.67	0.16	0.25	0	1.99	0.82
Aleatoric Velocity	0.71	0.19	0.31	0.18	0.03	0	0.49	0.17
Epistemic Velocity	4.08	0.49	1.46	0.64	0.39	0.02	3.01	0.30

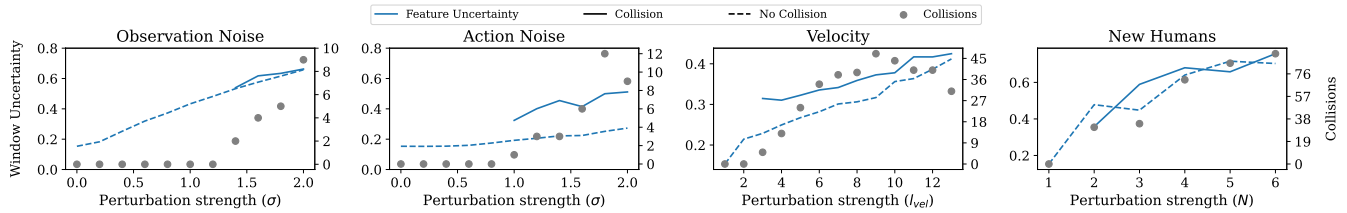


Fig. 6: Windowed predictive uncertainty of features extractor using MC-dropout approach on step before collision or at closest distance.

3) *Uncertainty-Aware Action Selection*: For collision avoidance, the uncertainty estimates are used for a POC estimation using (10) with the threshold constants for MC-dropout $\lambda_{ep} = 0.03$, $\lambda_f = 0.3$, $\lambda_{prox} = 0.9$, $\beta_1 = 0.5$ and deep ensemble $\lambda_{ep} = 0.08$, $\lambda_f = 0.0033$, $\lambda_{prox} = 0.9$, $\beta_1 = 0.5$. The parameters are identified by analyzing uncertainty-perturbation correlations, e.g. Fig. 3 and Fig 6. This ensures that the safe action selection only activates in steps or scenarios with a high risk of collision. The results show that the MC-dropout is more suitable for safe action selection across all perturbations and strengths as aggregated in Table IV with the relative percentage of prevented collisions compared to no safe action selection.

TABLE IV: Percentage of prevented collisions with safe action selection.

Approach	Obs. Noise	Action Noise	Velocity	More Humans
MC-dropout	100 ± 0	6 ± 5	56 ± 2	81 ± 8
Ensemble	79 ± 11	0 ± 0	16 ± 1	59 ± 13

C. Discussion

In social navigation, human safety is influenced by physical aspects (e.g. collisions) and psychological aspects (e.g. discomfort). Our reward formulation accounts for both and thus maximizing the reward also improves the safety in both aspects. Using dropout and ODV in PPO leads to better policy quality in terms of training convergence, evaluation, and generalization performance. With a higher success rate and a lower collision rate, the ODV-PPO with dropout approach is also safer by design. In addition, the augmentation with ODV enables the disentangling of the uncertainty, which allows the use of additional safety measures. The circle interaction scenario with staged interaction has the least stochasticity in position sampling but leads to good generalization, faster training convergence, and lower training variance across all investigated algorithms. The generalisation for the ODV-PPO with dropout in the circle interaction scenario is not as good as for the policy trained in the random scenario, but for all other algorithms it is good as well. This opens the research question of whether the staged interaction in training can support generalization while leading to fast convergence. Nevertheless, if the scenario distribution differs from the training distribution, the performance decreases, and the policy predicts overconfident actions. However, a predictive uncertainty does not necessarily correlate with high uncertainty in decision-making as visualized in Fig. 4 but can reveal risky scenarios. This further confirms the need for disentangling uncertainty estimates in policy distribution and not only to detect novel scenarios or predictive uncertainty. The comparison of the uncertainty methods

shows that the MC-dropout approach can better distinguish between aleatoric and epistemic uncertainty with properly selected dropout rate in inference and has additionally higher sensitivity to noise. The aleatoric uncertainty is sensitive to noises, showing that it associates the uncertainty type with the source of uncertainty. However, since all perturbed scenarios are partially OOD scenarios and the policy was only trained in a very simple scenario, the epistemic uncertainty is generally high and correlates to aleatoric uncertainty. These results for disentangling uncertainty in DRL are similar to recent work on classification [34], aleatoric and epistemic uncertainty show correlation, but tailored methods can be used for specific applications. Furthermore, the results show that the perturbations sources have varying impacts on decision-making, whereas they impact equally in predictive uncertainty. The policy is more uncertain about the heading throughout all perturbations, which is crucial for safe action selection and future design of DRL policies. More humans in the environment cause the highest uncertainty in decision-making, but collisions are most difficult to prevent in the case of action noise. For safe action selection, the results show that it is possible to parametrize a threshold function for POC calculation to detect scenarios of high risk to prevent them. However, one downside of this approach is the manual parametrization, which requires a perturbation analysis in advance. Furthermore, if the uncertainty estimation method has low sensitivity for perturbation, it is more challenging for the POC as in the ensemble approach.

VI. CONCLUSIONS

This paper incorporated and disentangled epistemic, aleatoric, and predictive uncertainty estimation in a DRL policy with a safe action selection for perturbation robustness in social navigation. We integrated Observation-Dependent Variance (ODV) and dropout into the PPO algorithm with adaptations in the action network and loss function. This, and staged interaction in training scenarios, lead to a better generalization with faster convergence and enables disentangling the aleatoric and epistemic uncertainty in decision-making. The results show that the MC-dropout-based approach is superior for uncertainty estimation and, in combination with the proposed safe action selection, can avoid more collisions than the ensemble approach. In addition, the predictive uncertainty in perturbed environments can be high, although the robot is sure about selecting the action. Consequently, MC-dropout and ODV should be used to estimate the policy distribution uncertainty to detect when and why the robot is uncertain. Future works will develop sample-free methods.

REFERENCES

- [1] E. Alao and P. Martinet, "Uncertainty-aware navigation in crowded environment," in *17th International Conference on Control, Automation, Robotics and Vision (ICARCV)*. IEEE, 2022, pp. 293–298.
- [2] X. Sun, Q. Zhang, Y. Wei, and M. Liu, "Risk-aware deep reinforcement learning for robot crowd navigation," *Electronics*, 2023.
- [3] C. Mavrogiannis, F. Baldini, A. Wang, D. Zhao, P. Trautman, A. Steinfeld, and J. Oh, "Core challenges of social robot navigation: A survey," *ACM Transactions on Human-Robot Interaction*, 2023.
- [4] M. Golchoubian, M. Ghafurian, K. Dautenhahn, and N. L. Azad, "Uncertainty-aware drl for autonomous vehicle crowd navigation in shared space," 2024. [Online]. Available: <http://arxiv.org/pdf/2405.13969v1>
- [5] D. Flögel, L. Fischer, T. Rudolf, T. Schürmann, and S. Hohmann, "Socially integrated navigation: A social acting robot with deep reinforcement learning," in *2024 IEEE/RSJ International Conference on Intelligent Robots and Systems (IROS)*. IEEE, 2024.
- [6] K. Zhu and T. Zhang, "Deep reinforcement learning based mobile robot navigation: A review," *Tsinghua Science and Technology*, vol. 26, no. 5, pp. 674–691, 2021.
- [7] K. Ryu and N. Mehr, "Integrating predictive motion uncertainties with distributionally robust risk-aware control for safe robot navigation in crowds," 2024. [Online]. Available: <http://arxiv.org/pdf/2403.05081v1>
- [8] A. Sedlmeier, T. Gabor, T. Phan, and L. Belzner, "Uncertainty-based out-of-distribution detection in deep reinforcement learning," *Digitale Welt*, vol. 4, no. 1, pp. 74–78, 2020.
- [9] T. Fan, P. Long, W. Liu, J. Pan, R. Yang, and D. Manocha, *Learning Resilient Behaviors for Navigation Under Uncertainty*. Piscataway, NJ: ICRA, 2020.
- [10] M. Everett, B. Lutjens, and J. P. How, "Certifiable robustness to adversarial state uncertainty in deep reinforcement learning," *IEEE Transactions on Neural Networks and Learning Systems*, 2022.
- [11] H. Yang, C. Yao, C. Liu, and Q. Chen, "Rmrl: Robot navigation in crowd environments with risk map-based deep reinforcement learning," *IEEE Robotics and Automation Letters*, vol. 8, no. 12, 2023.
- [12] Y.-J. Mun, M. Itkina, S. Liu, and K. Driggs-Campbell, "Occlusion-aware crowd navigation using people as sensors," in *2023 IEEE International Conference on Robotics and Automation (ICRA)*, 2023.
- [13] W. R. Clements, B. van Delft, B.-M. Robaglia, R. B. Slaoui, and S. Toth, "Estimating risk and uncertainty in deep reinforcement learning," 2019. [Online]. Available: <http://arxiv.org/pdf/1905.09638v5>
- [14] B. Charpentier, R. Senanayake, M. Kochenderfer, and S. Günnemann, "Disentangling epistemic and aleatoric uncertainty in reinforcement learning," 2022. [Online]. Available: <https://arxiv.org/abs/2206.01558>
- [15] O. Lockwood and M. Si, "A review of uncertainty for deep reinforcement learning," in *Proceedings of the AAAI Conference on Artificial Intelligence and Interactive Digital Entertainment*, 2022.
- [16] J. Choi, C. Dance, J.-e. Kim, S. Hwang, and K.-s. Park, "Risk-conditioned distributional soft actor-critic for risk-sensitive navigation," in *2021 IEEE International Conference on Robotics and Automation (ICRA)*. IEEE, 2021, pp. 8337–8344.
- [17] K. Zhu, B. Li, W. Zhe, and T. Zhang, "Collision avoidance among dense heterogeneous agents using deep reinforcement learning," *IEEE Robotics and Automation Letters*, vol. 8, no. 1, pp. 57–64, 2023.
- [18] V. Narayanan, B. M. Manoghar, R. P. RV, and A. Bera, "Ewarent: Emotion-aware pedestrian intent prediction and adaptive spatial profile fusion for social robot navigation," in *2023 IEEE International Conference on Robotics and Automation (ICRA)*. IEEE, 2023.
- [19] T. Zhang, T. Qiu, Z. Pu, Z. Liu, and J. Yi, "Robot navigation among external autonomous agents through deep reinforcement learning using graph attention network," *IFAC-PapersOnLine*, 2020.
- [20] S. S. Samsani and M. S. Muhammad, "Socially compliant robot navigation in crowded environment by human behavior resemblance using deep reinforcement learning," *IEEE Robotics and Automation Letters*, vol. 6, no. 3, pp. 5223–5230, 2021.
- [21] M. Everett, Y. F. Chen, and J. P. How, "Collision avoidance in pedestrian-rich environments with deep reinforcement learning," *IEEE Access*, vol. 9, pp. 10357–10377, 2021.
- [22] J. Schulman, F. Wolski, P. Dhariwal, A. Radford, and O. Klimov, "Proximal policy optimization algorithms," 20.07.2017.
- [23] T. Haarnoja, A. Zhou, K. Hartikainen, G. Tucker, S. Ha, J. Tan, V. Kumar, H. Zhu, A. Gupta, P. Abbeel, and S. Levine, "Soft actor-critic algorithms and applications," 2018.
- [24] Antonin Raffin, Ashley Hill, Adam Gleave, Anssi Kanervisto, Maximilian Ernestus, and Noah Dormann, "Stable-baselines3: Reliable reinforcement learning implementations," *Journal of Machine Learning Research*, vol. 22, no. 268, pp. 1–8, 2021.
- [25] S. Yao, G. Chen, Q. Qiu, J. Ma, X. Chen, and J. Ji, "Crowd-aware robot navigation for pedestrians with multiple collision avoidance strategies via map-based deep reinforcement learning," in *2021 IEEE/RSJ International Conference on Intelligent Robots and Systems (IROS)*, 2021.
- [26] B. Brito, M. Everett, J. P. How, and J. Alonso-Mora, "Where to go next: Learning a subgoal recommendation policy for navigation among pedestrians," 25.02.2021.
- [27] Z. Hu, J. Pan, T. Fan, R. Yang, and D. Manocha, "Safe navigation with human instructions in complex scenes," *IEEE Robotics and Automation Letters*, vol. 4, no. 2, pp. 753–760, 2019.
- [28] B. Chen, H. Zhu, S. Yao, S. Lu, P. Zhong, Y. Sheng, and J. Wang, "Socially aware object goal navigation with heterogeneous scene representation learning," *IEEE Robotics and Automation Letters*, 2024.
- [29] J. Li, C. Hua, H. Ma, J. Park, V. Dax, and M. J. Kochenderfer, "Multi-agent dynamic relational reasoning for social robot navigation," 2024. [Online]. Available: <http://arxiv.org/pdf/2401.12275v1>
- [30] Z. Xie and P. Dames, "Drl-vo: Learning to navigate through crowded dynamic scenes using velocity obstacles," *IEEE Transactions on Robotics*, 2023.
- [31] B. P. Charpentier, "Uncertainty estimation for independent and non-independent data," Ph.D. dissertation, Technische Universität München, 2024.
- [32] Y. Gal and Z. Ghahramani, "Dropout as a bayesian approximation: Representing model uncertainty in deep learning," 2015.
- [33] Y. Gal, "Uncertainty in deep learning," 2016. [Online]. Available: <https://api.semanticscholar.org/CorpusID:86522127>
- [34] B. Mucsányi, M. Kirchhof, and S. J. Oh, "Benchmarking uncertainty disentanglement: Specialized uncertainties for specialized tasks," 2024. [Online]. Available: <http://arxiv.org/pdf/2402.19460v2>
- [35] M. Ghavamzadeh, S. Mannor, J. Pineau, and A. Tamar, "Bayesian reinforcement learning: A survey," *Foundations and Trends® in Machine Learning*, vol. 8, no. 5-6, pp. 359–483, 2015.
- [36] Björn Lütjens, M. Everett, and J. P. How, "Safe reinforcement learning with model uncertainty estimates," in *2019 International Conference on Robotics and Automation (ICRA)*, 2019, pp. 8662–8668.
- [37] G. Kahn, A. Villaflor, V. Pong, P. Abbeel, and S. Levine, "Uncertainty-aware reinforcement learning for collision avoidance," 2017. [Online]. Available: <http://arxiv.org/pdf/1702.01182v1>
- [38] M. Hausknecht and N. Wagnen, "Consistent dropout for policy gradient reinforcement learning," 2022. [Online]. Available: <http://arxiv.org/pdf/2202.11818v1>
- [39] J. Rios-Martinez, A. Spalanzani, and C. Laugier, "From proxemics theory to socially-aware navigation: A survey," *International Journal of Social Robotics*, vol. 7, no. 2, pp. 137–153, 2015.
- [40] C. Diehl, T. Sieverich, M. Krüger, F. Hoffmann, and T. Bertram, "Umbrella: Uncertainty-aware model-based offline reinforcement learning leveraging planning," *arXiv preprint arXiv:2111.11097*, 2021.
- [41] L. Kästner, J. Li, Z. Shen, and J. Lambrecht, "Enhancing navigational safety in crowded environments using semantic-deep-reinforcement-learning-based navigation," 2021. [Online]. Available: <http://arxiv.org/pdf/2109.11288v1>
- [42] C. Richter and N. Roy, "Safe visual navigation via deep learning and novelty detection," *Robotics: Science and Systems XIII*, 2017.
- [43] Y. F. Chen, M. Liu, M. Everett, and J. P. How, "Decentralized non-communicating multiagent collision avoidance with deep reinforcement learning," in *2017 IEEE International Conference on Robotics and Automation (ICRA)*. IEEE, 2017, pp. 285–292.
- [44] E. T. Hall, *The hidden dimension*. New York: Anchor Books, 1996.
- [45] C. Kim, J.-K. Cho, H.-S. Yoon, S.-W. Seo, and S.-W. Kim, "Unicon: Uncertainty-conditioned policy for robust behavior in unfamiliar scenarios," *IEEE Robotics and Automation Letters*, 2022.
- [46] J. van den Berg, S. J. Guy, M. Lin, and D. Manocha, "Reciprocal n-body collision avoidance," in *Robotics Research*, ser. Springer Tracts in Advanced Robotics. Springer Berlin Heidelberg, 2011.
- [47] A. Francis and et.al., "Principles and guidelines for evaluating social robot navigation algorithms," 2023. [Online]. Available: <http://arxiv.org/pdf/2306.16740v4>
- [48] T. Akiba, S. Sano, T. Yanase, T. Ohta, and M. Koyama, "Optuna: A next-generation hyperparameter optimization framework," in *Proceedings of the 25th ACM SIGKDD International Conference on Knowledge Discovery and Data Mining*, 2019.